Available online at www.sciencedirect.com

SciVerse ScienceDirect

Ceramics International 39 (2013) 3979–3986

CERAMICS INTERNATIONAL

www.elsevier.com/locate/ceramint

The PZT system ($PbTi_xZr_{1-x}O_3$, $0 \le x \le 1.0$): Dielectric response of solid solutions in broad temperature ($10 \le T \le 1000$ K) and frequency ($10^{-2} \le f \le 10^7$ Hz) ranges (Part 4)

I.N. Andryushina*[,1], L.A. Reznichenko, I.M. Shmytko, L.A. Shilkina, K.P. Andryushin, Yu.I. Yurasov, S.I. Dudkina

Research Institute of Physics, Southern Federal University, Stachki street, 194, Rostov-on-Don 344090, Russia

Received 5 October 2012; accepted 23 October 2012
Available online 10 November 2012

Abstract

Solid solution (SS) ceramics of the PZT ($PbTi_xZr_{1-x}O_3$, $0 \le x \le 1.0$) system were studied in broad temperature ($10 \le T \le 1000$ K) and electric field frequency ($10^{-2} \le f \le 10^7$ Hz) ranges. Several groups of SS were distinguished, which differ by nonmonotonic behavior of dielectric parameters in the cryogenic temperature range and at $T > 300$ K, which results both from the defective state and from the polymorphism of SS. A conclusion is made on the expediency of use of the obtained data during the application of materials based on the PZT system in the broad range of external actions.

Keywords: D. PZT; Dielectric response; Broad temperature; Polymorphism

1. Introduction

Among the prominent classes of electrically active media particular interest present solid solutions (SS) of the binary system $(1-x)PbZrO3-xPbTiO_3$ (PZT), which became the basis of almost all industrially produced functional materials. The study of physicotechnical properties of these SS, which continues for decades already, revealed a broad spectrum of experimental potential, which is in many respects determined by a special phase diagram of this system. It was shown recently [1] that some of its fragments are formed at ultra low temperatures. The results of the dielectric properties studies of SS in this temperature range are presented in very few papers and were performed in a restricted frequency range and for selected compositions only [2,3].

Thus, of current importance is a detailed study of dielectric response of SS of this system in broad temperature and frequency ranges, which is the aim of the present study.

2. Objects under study, synthesis and measurement methods

The objects under study are SS of $PbTi_xZr_{1-x}O_3$ with $0.0 \le x \le 1.0$. Their synthesis methods are described in detail in [4].

Low-temperature dielectric measurements were performed in the temperature interval 10–300 K at frequencies 20–5×10^6 Hz using sensitive impedance analyzer Wayne Kerr 6500B. The samples were cooled using closed cycle helium refrigerator cryostat CCS-150 (Cryogenics). The temperature control was performed using the temperature controller LakeShore 331, which allows maintaining the given temperature with the accuracy of ± 0.01 K. During measurement the samples were located in the vacuum chamber of the cryostat, the vacuum was created by turbomolecular pump Boc Edwadrs. The dielectric spectra were studied in the temperature range 160–300 K at 16 frequencies from the interval $10^{-2} \times 10^7$ Hz using multipurpose

*Corresponding author. Tel.: +78632434066.
E-mail address: futur6@mail.ru (I.N. Andryushina).
[1]Mailing address: Stachki ave, 194, Rostov-on-Don, 344090, Russian Federation.

0272-8842/$ - see front matter © 2012 Elsevier Ltd and Techna Group S.r.l. All rights reserved.
http://dx.doi.org/10.1016/j.ceramint.2012.10.246

measuring bridge Novocontrol ALPHA high-resolution dielectric analyzer, equipped with the Novocontrol QUATRO cryosystem for low-temperature measurements.

High-temperature dielectric spectra were studied by the home-made measuring bench using the immittance measuring device E7-20. The measurements were performed in the temperature interval 300–1000 K and the frequency range 25–10^6 Hz.

Low-temperature x-ray measurements were conducted in the helium cryostat developed by the Institute of solid sated physics of RAS (Chernogolovka, Russia), which allows thermostating the sample in the range 4.2–300 K with precision of 0.05–0.1 K. The measurements were performed using D500 (Siemens) x-ray diffractometer utilizing monochrome Cu-K_α radiation.

3. Experimental results and discussion

Fig. 1 shows the most characteristic temperature (T) dependencies of the real ($\varepsilon'/\varepsilon_0$) and imaginary ($\varepsilon''/\varepsilon_0$) parts of the relative dielectric permittivity at different frequencies (f) of the measuring electric field. The behavior patterns of $\varepsilon'/\varepsilon_0$ (T) allows distinguishing 11 concentration ranges, represented by 11 groups:

1. ($0.00 < x \leq 0.13$)—upon increasing temperature $\varepsilon'/\varepsilon_0$ increases with rate changing at 155–160 K; the values of $\varepsilon'/\varepsilon_0$ are relatively small (150–400 in the interval 10–300 K); no maximum of $\varepsilon'/\varepsilon_0(T)$ is formed; $\varepsilon''/\varepsilon_0$ possesses diffuse maximum at the inflection point of $\varepsilon'/\varepsilon_0$ (T);
2. ($0.13 < x \leq 0.16$)—for $T < 270$ K the $\varepsilon'/\varepsilon_0(T)$ dependencies are similar to those of SS of group 1; in the vicinity of 270–300 K a small maximum begins to form in the $\varepsilon'/\varepsilon_0(T)$ dependencies; $\varepsilon''/\varepsilon_0$ is non-monotone with a diffuse maximum occupying almost the whole temperature range, which is apparently a result of merging of two maxima: one at ~130 K and another one in the vicinity of the high-temperature $\varepsilon'/\varepsilon_0$ maximum at 270–300 K;
3. ($0.16 < x \leq 0.26$)—the $\varepsilon'/\varepsilon_0$ (T) dependencies are similar to those of SS of the groups 1 and 2 for $T < 250$ K, but at $T = 250$–300 K a small "plateau-like" region is formed, where $\varepsilon'/\varepsilon_0$ is almost constant; $\varepsilon''/\varepsilon_0$ is characterized by a pronounced maximum at $T \sim 230$–240 K, i.e.,

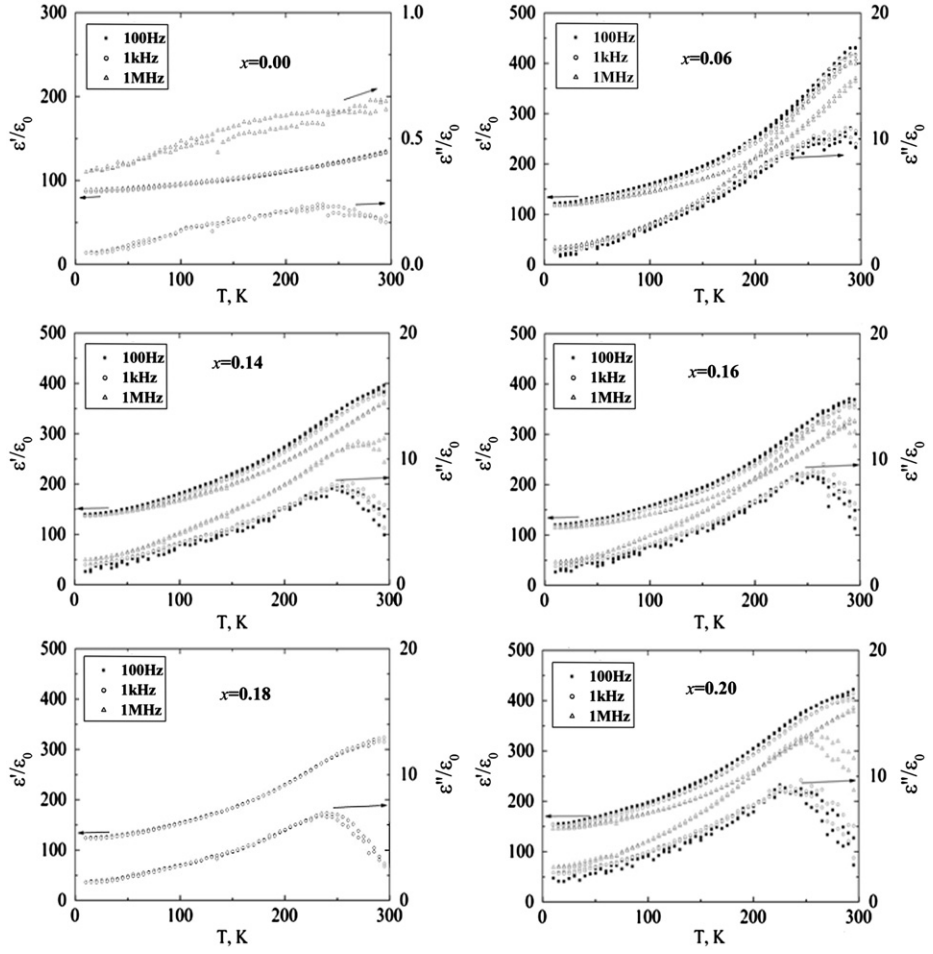

Fig. 1. Temperature dependencies of the real and imaginary parts of dielectric constant (in the interval 10–300 K) of SS of the PZT system (in the heating and cooling runs).

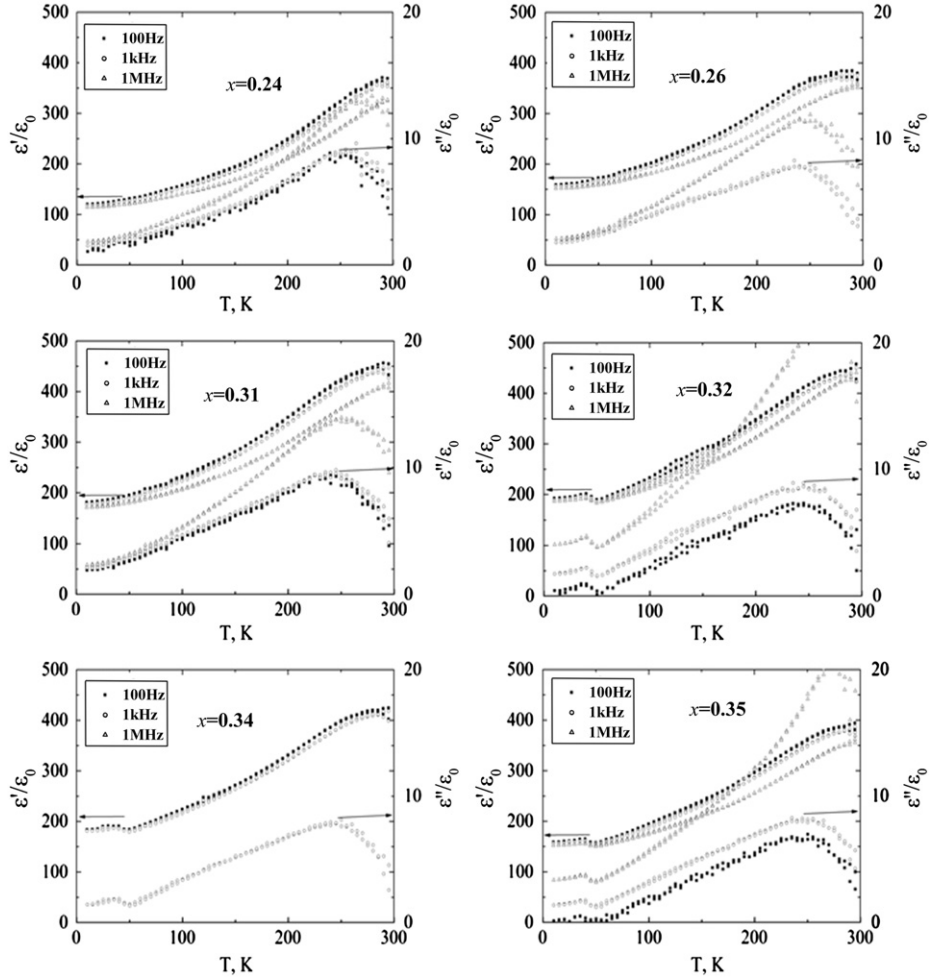

Fig. 1. Continued.

approximately where the "plateau" begins to form in the $\varepsilon'/\varepsilon_0(T)$ dependencies;

4. $(0.26 < x \leq 0.31)$—upon increasing temperature the $\varepsilon'/\varepsilon_0$ dependencies in this group change increasing rate already at 130–140 K; this group is characterized by a maximum forming in the $\varepsilon'/\varepsilon_0(T)$ dependencies at ~260–270 K; the $\varepsilon''/\varepsilon_0$ (T) dependencies are analogous to those of SS from group 2;
5. $(0.31 < x \leq 0.35)$—in this concentration interval at temperatures 25–55 K distinct low-temperature anomalies (maxima) of $\varepsilon'/\varepsilon_0$ are observed; upon increasing temperature $\varepsilon'/\varepsilon_0$ rises and forms a maximum at 270–300 K; the $\varepsilon''/\varepsilon_0$ (T) dependencies are characterized by anomalous behavior at the temperatures of anomalies of $\varepsilon'/\varepsilon_0$;
6. $(0.35 < x \leq 0.42)$—the SS of this group possess no low-temperature maximum of $\varepsilon'/\varepsilon_0$; in the vicinity of 300 K a plateau-like region is formed as for SS of group 3, which upon $PbTiO_3$ content increase broadens and begins to form already at 250 K; the $\varepsilon''/\varepsilon_0$ (T) dependencies are similar to those of SS from group 3;
7. $(0.42 < x \leq 0.47)$—in this group the rate of increase of $\varepsilon'/\varepsilon_0$ changes at 50 K and a first inflection point appears; at ~100–110 K a second inflection point forms in the $\varepsilon'/\varepsilon_0(T)$ dependencies; at 225–250 K a "step-like" anomaly is observed with subsequent rise of $\varepsilon'/\varepsilon_0$; the $\varepsilon''/\varepsilon_0$ (T) dependencies in the interval 10–150 K are almost linear; subsequent temperature increase to 200 K is accompanied by $\varepsilon''/\varepsilon_0$ slope change;
8. $(0.47 < x \leq 0.52)$—it has to be noted that in this group increased values of $\varepsilon'/\varepsilon_0$ are observed (especially at $x=0.485$) compared to all SS of this system; all SS of this group are characterized by a change of the rate of increase of $\varepsilon'/\varepsilon_0$ in the low-temperature range at 30–40 K; further temperature increase results in $\varepsilon'/\varepsilon_0$ increase and in formation of a diffuse maximum, the lower bound of which shifts towards lower temperature depending on composition (for example, in the SS with $x=0.485$ the lower bound of the diffuse maximum is formed at 200 K; in the SS with $x=0.495$ the lower bound shifts and forms already at 100 K; upon increase of concentration up to $x=0.515$ the lower bound is formed already at 75 K); thus, the width of the maximum of the first SS is 50 K, of the second—150 K, and of the third—175 K; the $\varepsilon''/\varepsilon_0(T)$ dependencies are almost linear in the intervals: 10–150 K for SS with $x=0.485$, 10–100 K for SS with $x=0.495$,

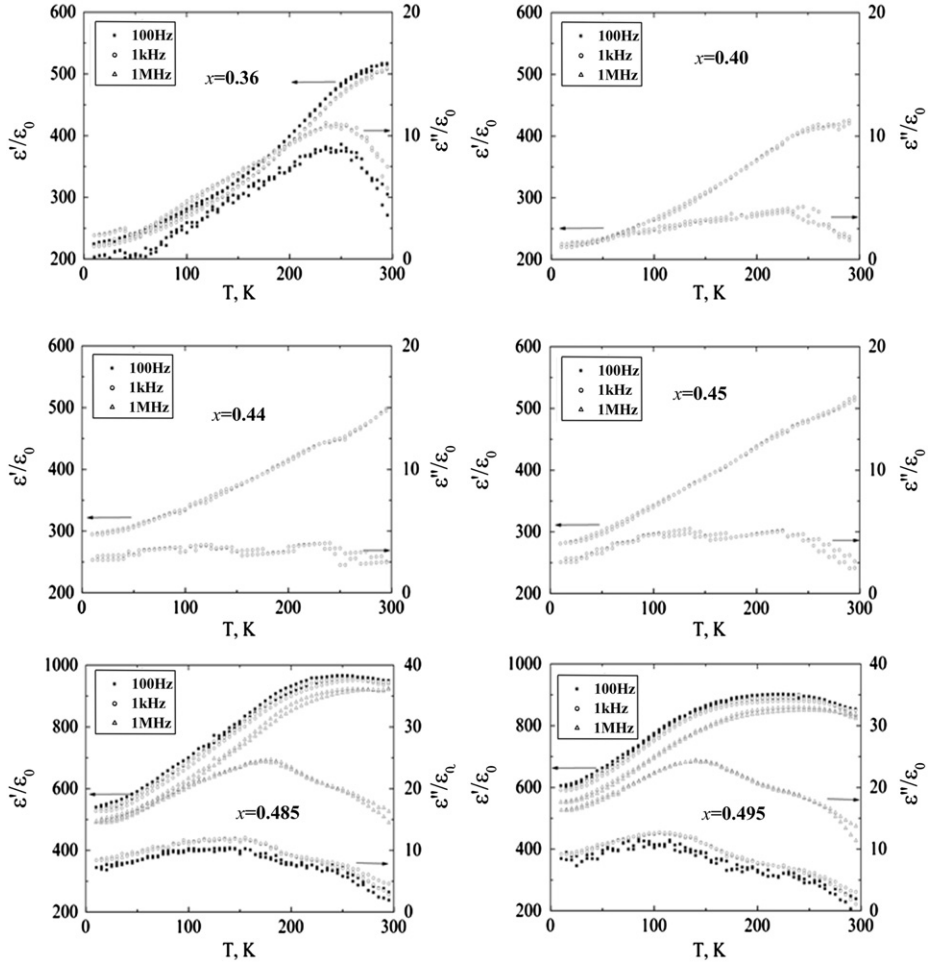

Fig. 1. Continued.

and 10–75 K for SS with $x=0.515$; upon further temperature increase $\varepsilon''/\varepsilon_0$ decreases with different rates (first rapidly and slowly afterwards), forming inflection points in the $\varepsilon''/\varepsilon_0$ (T) dependencies at 225 K for SS with $x=0.485$ and $x=0.495$ and at 200 K for SS with $x=0.515$;

9. ($0.52 < x \leq 0.57$)—the SS of this group are characterized by changing rate of $\varepsilon'/\varepsilon_0$ (T) in the low-temperature region at 20 K; upon temperature increase a distinct maximum is formed at 250 K; the $\varepsilon''/\varepsilon_0$ (T) dependencies are similar to those of SS of group 8, but the change of slope of $\varepsilon''/\varepsilon_0$ appears at 160 K;
10. ($0.57 < x \leq 0.70$)—the SS of this group are characterized by almost linear dependencies of $\varepsilon'/\varepsilon_0$, however in the low-temperature range in the vicinity of 30 K an inflection point of $\varepsilon'/\varepsilon_0$ is observed; upon temperature increase up to 160 K a second inflection point of $\varepsilon'/\varepsilon_0$ appears; the $\varepsilon''/\varepsilon_0$ (T) dependencies experience a maximum close to 150 K, approximately at the place of the second inflection point;
11. ($0.70 < x \leq 1.00$)—the $\varepsilon'/\varepsilon_0$ (T) dependencies of this group are almost linear up to 250 K; upon further temperature increase a rapid rise of $\varepsilon'/\varepsilon_0$ occurs, which is induced by defects due to degradation of $PbTiO_3$.

Of special importance are the results obtained for SS with $x=0.495$–0.510, which are located close to the morphotropic region, where the maxima of $\varepsilon'/\varepsilon_0$ recur in the direct and backward runs and are frequency dependent. These SS were studied by us in a broader frequency range with a bigger number of measuring frequencies.

Fig. 2 shows temperature dependencies of $\varepsilon'/\varepsilon_0$ in the interval 100–300 K at different measuring frequencies f. The compositions with $x=0.495$ and $x=0.505$ show diffuse maxima at $T=230$–260 K, which slightly change their position depending on x. For $x=0.51$ an analogous maximum is formed at 150–160 K, whereas the higher-temperature ($\sim$230 K) process gradually decays. The main peculiarity of these maxima is their shift towards higher temperatures, the decrease and smearing of the peak value $\varepsilon'/\varepsilon_{0m}$ with increasing f. The dispersion depth of $\varepsilon'/\varepsilon_{0m}$ of SS with $x=0.495$ and 0.505 is $\Delta\varepsilon'/\varepsilon_{0m} \approx (\sim 13.5)\%$, whereas of SS with $x=0.51$—$\Delta\varepsilon'/\varepsilon_{0m} \approx (\sim 44.8)\%$, where $\Delta\varepsilon'/\varepsilon_{0m} = [(\varepsilon'/\varepsilon_{0m0.01\ Hz} - \varepsilon'/\varepsilon_{0m5\ MHz})/\varepsilon'/\varepsilon_{0m0.01\ Hz}] \times \bullet 100\%$. The studies have shown, that the dependences of temperature of maxima (T_m) of $\varepsilon'/\varepsilon_0$ on frequency in the Arrhenius coordinates are not linear, i.e., are not described by the Arrhenius law, which evidences of non-Debye character of dielectric relaxation in these materials. At the same time the frequency dependence of

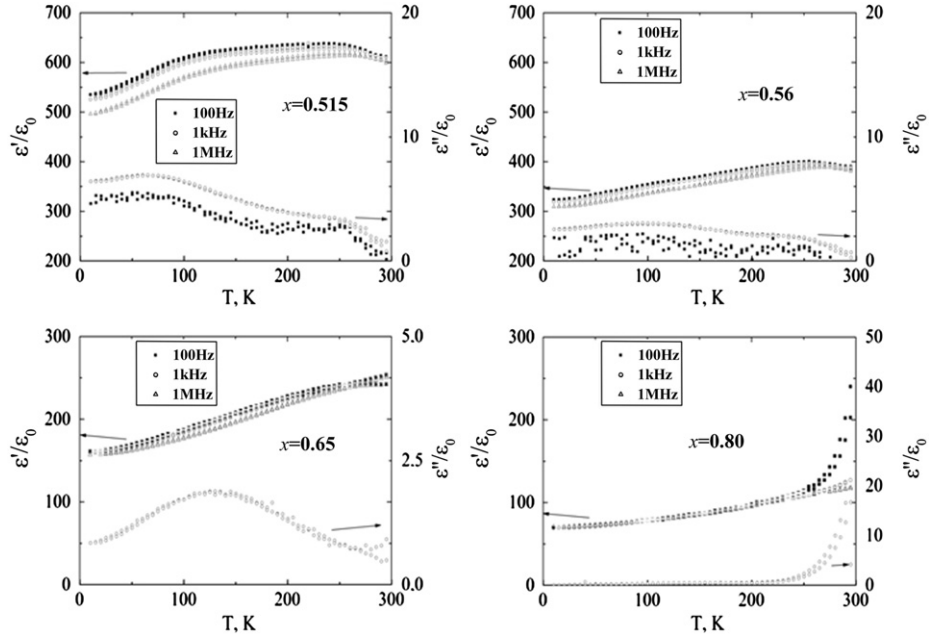

Fig. 1. Continued.

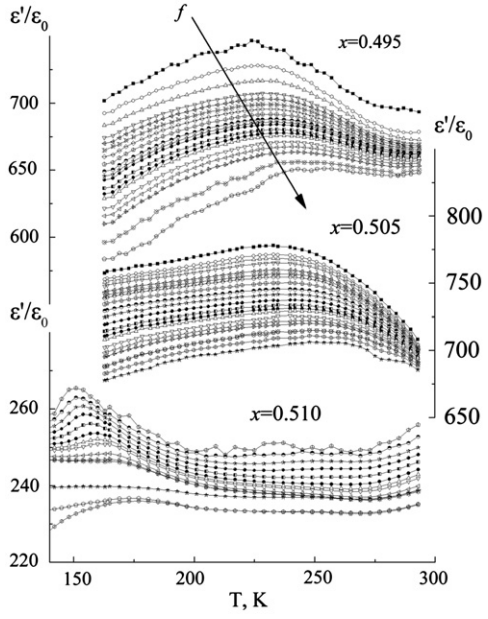

Fig. 2. Temperature dependencies of the dielectric constant of the PZT system SS with $x=0.495$–0.510 at different frequencies.

the temperatures of maxima of $\varepsilon'/\varepsilon_0(T)$ is well described by the Vogel–Fulcher law $f=f_0\exp\times[-E_a/k(T_m-T_0)$, where f_0 is the frequency of attempts of potential barrier crossing, E_a is the activation energy of the process, k is the Boltzmann constant, T_m is the temperature of maximum, and T_0 is the Vogel–Fulcher temperature, which is interpreted as the temperature of "static freezing" of electric dipoles or as the transition temperature to the dipole glass state. For all the studied SS $f_0\sim1\times10^{11}$ Hz, which is close to the values of f_0 for classic relaxor ferroelectrics. The value E_a for $x=0.495$ and 0.505 is ≈0.008 eV, whereas for SS with $x=0.51$—$E_a\approx0.01$ eV.

For the description of the dielectric permittivity spectra in the complex plane a generalized Debye model suggested by Cole–Cole [5] is used, with frequency dependent complex dielectric permittivity $\varepsilon*$ represented by

$$\varepsilon^*=\varepsilon_\infty+\frac{\Delta\varepsilon}{1+(i\omega\tau)^{1-\alpha}},\quad(1)$$

where ε_∞ is the dielectric permittivity in the high-frequency limit, which shifts the arc along the real axis, $\Delta\varepsilon=\varepsilon_s-\varepsilon_\infty$ is the chord length of the semicircular arc, ε_s is the static dielectric permittivity, and τ is the middle point of the distribution of relaxation times denoted by Cole–Cole (model) when the α parameter is related to its width.

Fig. 3 shows Cole–Cole diagrams for $x=0.495$ and 0.505 according to experimental data. Upon approximation of experimental data the main parameters shown in Table 1 for $x=0.495$ and 0.505 were obtained. Two semi-circles appear in the Cole–Cole diagram with centers on the $\varepsilon''/\varepsilon_0$ axis evidencing of two relaxation processes with different times τ_1 and τ_2, which may be related to formation of new phases as well as to the defective structure of samples and will be studied in detail later.

In order to clarify the relaxation mechanism in these SS low-temperature x-ray studies were conducted.

Fig. 4 shows the temperature dependencies of $\varepsilon'/\varepsilon_0$ (at various frequencies from the interval 100 to 10^5 Hz), interplanar spacings ($d_{(2\,0\,0)}$, $d_{(0\,0\,2)}$), and half-widths $B_{(2\,0\,0)}$ of x-ray (tetragonal) diffraction lines. The arrows show the regions of anomalous behavior of parameters. The interval 10–40 K is characterized by a change in the rate of increase of $\varepsilon'/\varepsilon_0$. In the ascending part of $\varepsilon'/\varepsilon_0$ special points (130, 155, and 210 K) are discerned, at which

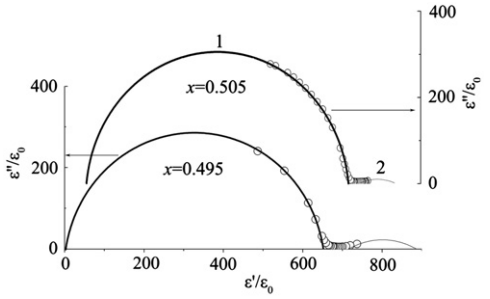

Fig. 3. Cole–Cole diagrams obtained for $x=0.495$ and 0.505 at $T=200$ K. Notation: –○– – experimental data, —— – approximation curves.

Table 1
Calculated static (ε_s) and high-frequency (ε_∞) dielectric constants, the depth of the relaxation spectrum ($\varepsilon_\sigma-\varepsilon_\infty$), parameters of the relaxation time distribution (α, β) and the most probable relaxation time (τ) for various concentrations (x) in the relaxor region.

x		ε_s	ε_∞	$\varepsilon_\sigma-\varepsilon_\infty$	α	β	τ
0.495	1	663	236	427	0.2	1	1×10^{-8}
	2	1539	698	841	0.38	1	4.2×10^{-4}
0.505	1	708	10	698	0.06	1	1×10^{-7}
	2	824	744	80	0.72	1	1.2×10^{-4}

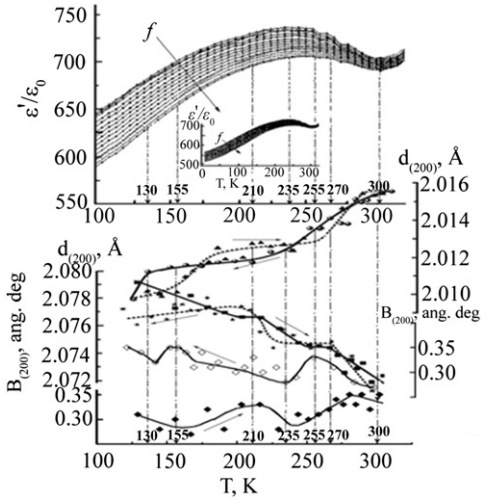

Fig. 4. Temperature dependencies of the dielectric constant $\varepsilon'/\varepsilon_0$ at different frequencies f of the measuring field, interplanar spacings ($d_{(2\,0\,0)}$, $d_{(0\,0\,2)}$), and half-widths B of the diffraction lines at $x=0.495$ (arrows indicate regions of anomalous behavior of parameters).

the slope of the curve changes. In the vicinity of ~235 K a relaxation maximum is formed. In the descending part of $\varepsilon'/\varepsilon_0$ at 255 K a local minimum is observed, whereas at 270 K the slope of $\varepsilon'/\varepsilon_0$ changes and the subsequent temperature increase leads to formation of a minimum at 300 K, after which increase of $\varepsilon'/\varepsilon_0$ occurs. It should be noted that the structural characteristics also experience anomalies at these temperatures. Thus, a strong correlation is observed between the changes in $\varepsilon'/\varepsilon_0$ and the structural parameters of the sample.

Due to the fact that no additional phases are observed in the low-temperature region by x-ray studies, it is probable, that the dielectric behavior is influenced by changes in the valence states of Pb, Ti, and Zr [6], which strengthen upon interaction with water and hydroxyl groups present in the samples. Another factors are polymorphic transformations of oxygen (α-phase (monoclinic cell with $a=5.403$ Å, $b=3.429$ Å, $c=5.086$ Å, $\beta=132.53^\circ$) $\overset{23.65K}{\longrightarrow}$ β-phase (rhombohedral cell with $a=4.21$ Å, $\alpha=46.25^\circ$) $\overset{43.65K}{\longrightarrow}$ γ-phase (cubic cell with $a=6.83$ Å) [7–9]) and ZrO_2, with the latter determined by adsorption of water molecules onto the surface of the particles of synthesized powders and ceramics [10]. As it was established in [10], high-temperature transformations of ZrO_2 may also occur close to room temperature due to nonstoichiometric oxygen vacancies and local strains related to them, which stabilize high-temperature phases.

According to the dielectric behavior in the high-temperature region the solid solutions can be divided into 5 groups (their representatives are shown in Fig. 5), differing in the dispersion character: the first group ($0.00<x\leq0.12$) is characterized by absence of dispersion before and at the phase transition (PT) (Fig. 5a), in the second group ($0.12<x\leq0.37$) weak dispersion before and appreciable at and after the PT is observed (Fig. 5b), the third group ($0.37<x\leq0.43$) is characterized by strong dispersion in the whole temperature range (Fig. 5c), and in the fourth ($0.43<x\leq0.505$) (Fig. 5d) and the fifth ($0.505<x<1.00$) (Fig. 5e) groups strong low-frequency dispersion is observed, which prevents formation of the maximum of $\varepsilon'/\varepsilon_0$ at T_C. The observed behavior is related to the following factors: to the specific character of $PbZrO_3$—an antiferroelectric, in which restructuring of antiparallel domains is practically impossible, to the movement of various interphase boundaries, to the increased imperfection of heterophase SS in the vicinity of MR, and to the peculiarities of $PbTiO_3$, which is inclined to self-destruction due to large internal mechanical stresses. The dispersion of $\varepsilon'/\varepsilon_0$ above the PT is determined by the three main causes: due to the movement of defects forming at the PT from the cubic to the low-symmetry phase (at high T), due to the clusters of the latter forming in the praphase, and due to the vacancies forming upon reduction of ions with variable valence (mainly of Ti). A series of anomalies of $\varepsilon'/\varepsilon_0(T)$ at $T\leq573$ K is in good correlation with PT's taking place at these temperatures (R(Pba2)→Rh(R3c)→Rh(R3m), where R is the rhombic phase; Rh are the low and high temperature rhombohedral phases, respectively).

4. Conclusions

1. Several groups of SS were distinguished differing by non-monotone behavior of dielectric parameters in the cryogenic temperature region, which is determined by defects. The relaxation processes are well described by the Vogel-Fulcher law, whereas the dielectric spectra

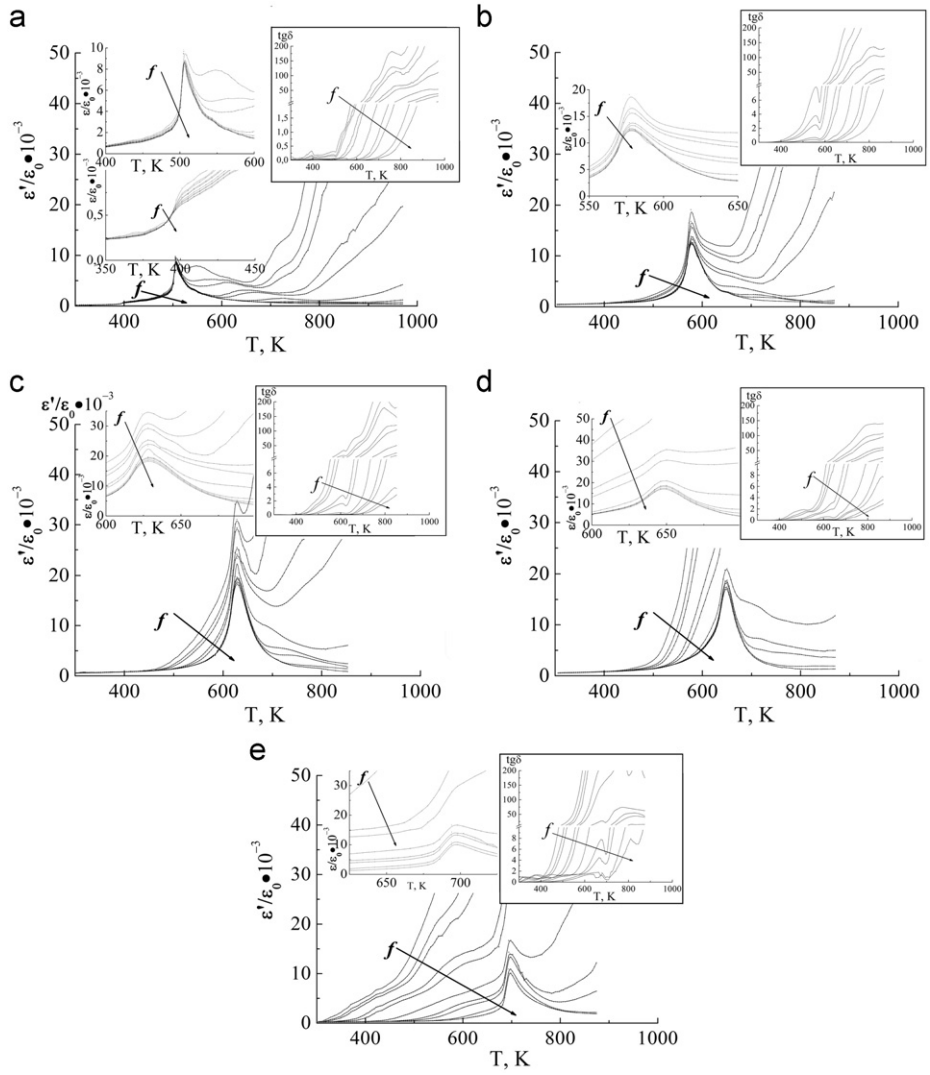

Fig. 5. $\varepsilon'/\varepsilon_0\,(T)$ of the PZT system SS at different frequencies f of the measuring electric field. The insets give $\varepsilon'/\varepsilon_0\,(T)|_f$ and tg $\delta(T)|_f$ in the vicinity of PT to the paraelectric phase.

by the Cole–Cole formula. A correlation between the relaxation process and the changes in structural characteristics of the $PbTi_{0.495}Zr_{0.505}O_3$ SS in the temperature interval 100–300 K is revealed.

2. A series of peculiarities of dispersion properties of SS of the PZT system at $T=300$–1000 K is discovered, which allowed isolating five concentration groups of SS ($0.00 < x \le 0.12$, $0.12 < x \le 0.37$, $0.37 < x \le 0.43$, $0.43 < x \le 0.505$, and $0.505 < x < 1.00$), differing in temperature-frequency behavior. The behavior of each group was given an interpretation. It is established that the dispersion of ε' in the vicinity of PT is determined by three main causes, each of which dominates in its own temperature and concentration interval and is related to the movement of defects forming at the PT from the cubic to low-symmetry phase (at high T), to the clusters of the latter, forming in the prophase, and to the vacancies forming due to reduction of ions with variable valence (mainly of Ti).

The obtained results are expedient to use during development of materials based on the PZT system intended to function in different temperature and frequency intervals.

Acknowledgments

We appreciate the help of Nikita Ter-Oganessian with the preparation of the manuscript. This work was financially supported by the Ministry of Education and Science of the Russian Federation, State contract No 16.513.11.3032.

References

[1] B. Noheda, Structure and high-piezoelectricity in lead oxide solid solutions, Current Opinion Solid State Mater. Science 6 (2002) 27–34.

[2] S.K. Ragini, D. Mishra, H. Pandey, G. Lemmens, Tendeloo Van, Evidence for another low-temperature phase transition in tetragonal $Pb(Zr_xTi_{1-x})O_3$ ($x=0.515$, 0.52), Physical Review B 64 (5) (2001) 0541011–0541016.

[3] A.A. Bokov, X. Long, Z.-G. Ye, Optically isotropic and monoclinic ferroelectric phases in $Pb(Zr_{1-x}Ti_x)O_3$ (PZT) single crystals near morphotropic phase boundary, Physical Review B 81 (2010) 172103.
[4] I.N. Andryushina, L.A. Reznichenko, V.A. Alyoshin, L.A. Shilkina, et al., The PZT system ($PbZr_{1-x}Ti_xO_3$, $0.0 \le x \le 1.0$): specific features of recrystallization sintering and microstructures of solid solutions, Ceramics International (2012).
[5] K.S. Cole, R.H. Cole, Dispersion and absoption in dielectrics, Journal of Chemical Physics 9 (4) (1941) 341–351.
[6] J. Frantti, S. Ivanov, S. Eriksson, H. Rundlöf, V. Lantto, J. Lappalainen, M. Kakihana, Phase transitions of $Pb(Zr_xTi_{1-x})O_3$ ceramics, Physical Review B 66 (6) (2002) 641081–6410815.
[7] C.S. Barrett, L. Meyer, J. Wasserman, Antiferromagnetic and crystal structure of alpha-oxygen, Journal of Chemical Physics 47 (1967) 592–597.
[8] E.M. Hoerm, Structure and imperfections of solid beta-oxygen, Acta Crystal 15 (1962) 845.
[9] D.E. Cox, E.J. Samuelsen, K.H. Beckurts, Neutron diffraction determination of the crystal structure and magnetic form factor of gamma-oxygen, Physical Review B 7 (7) (1973) 3102–3111.
[10] V.I. Alekseenko, G.K. Volkova, An adsorption mechanism underlying phase transformation in stabilized zirconia, Technical Physics 45 (9) (2000) 1154–1158.